New Phytologist **Supporting Information**
Article title: Pragmatic hydraulic theory predicts stomatal responses to climatic water deficits

Authors: John S. Sperry, Yujie Wang, Brett T. Wolfe, D. Scott Mackay, William R. L. Anderegg, Nate G. McDowell and William T. Pockman

Article acceptance date: 13 May 2016

The following Supporting Information is available for this article:

Table S1 Data set parameters. The first 7 data sets from tropical trees averaged 17 measurement days spaced every 3–6 wk from November 2011 to July 2013. The *Juniperus* and *Pinus* data sets averaged 8 measurement days per 7 month growing season for 2007–2010.

Data set	**Vuln curve**[1]			**Soil**[2]						
	#	**b** MPa	**c**	**α** MPa^{-1}	**n**	**k**[3] kg $h^{-1}m^{-2}$	**G**[4] kg $h^{-1}m^{-2}$	**D**[5] kPa	**Predawn**[6] -MPa	**Midday**[7] -MPa
Annona hayesii, transitional dry	8	5	4.3	81.6	1.09	9.74(11.13)	344(370)	1.1(0.73)	1.3(0.93)	1.9(1.05)
Astronium graveolens, transitional dry	7	4.9	3.3	81.6	1.09	4.81(5.81)	242(167)	1.2(0.77)	0.9(0.37)	1.7(0.75)
Bursera simaruba, dry	2	1.4	5.8	602.0	1.48	20.8(28.3)	80(131)	2.1(0.71)	0.6(0.15)	0.7(0.22
Cavanillesia platanifolia, transitional dry	1	1.3	2.3	81.6	1.09	10.6(11.21)	175(216)	1.2(0.80)	0.5(0.16)	0.6(0.14)
Cojoba rufescens, transitional dry	9	5.3	2.7	81.6	1.09	5.4(4.14)	400(237)	1.2(0.71)	1.2(0.44)	2.0(0.68)
C. rufescens, dry	5	3.8	1.2	602.0	1.48	15.7(17.49)	534(417)	2.1(0.74)	1.4(0.88)	2.3(0.92)
Genipa americana, dry	3	2.7	1.3	602.0	1.48	10.5(8.13)	274(273)	2.0(0.67)	1.6(1.12)	2.0(1.02)
Juniperus monosperma	10	8.7	3.8	204.0	1.41	2.23(2.05)	57(57)	2.7(0.84)	3.4(1.95)	4.0(1.50)
Pinus edulis	4 6r	3.43 3.56r	1.65 4.07r	204.0	1.41	3.96(4.99)	77(87)	2.7(0.82)	2.1(0.88)	2.6(0.63)

[1]Weibull function b and c from Eqn 1 (stems); # refers to curve number in Fig. S1; 'r' denotes root curve available for *P. edulis*.
[2]van Genuchten α and n for Eqn 2.
[3]Soil-canopy hydraulic conductance, k (mean[sd]), estimated from E/ΔP, where ΔP is difference between predawn and midday P_{canopy}. Values were excluded when E or ΔP = 0, or when ΔP was negative.
[4]Canopy diffusive conductance, G (mean[sd]).
[5]Vapor pressure deficit, D (mean[sd]).
[6]Predawn P_{canopy} (mean[sd]).
[7]Midday P_{canopy} (mean[sd]).

Fig. S1 Weibull function vulnerability curves for the study species. Numbering as in Table S1

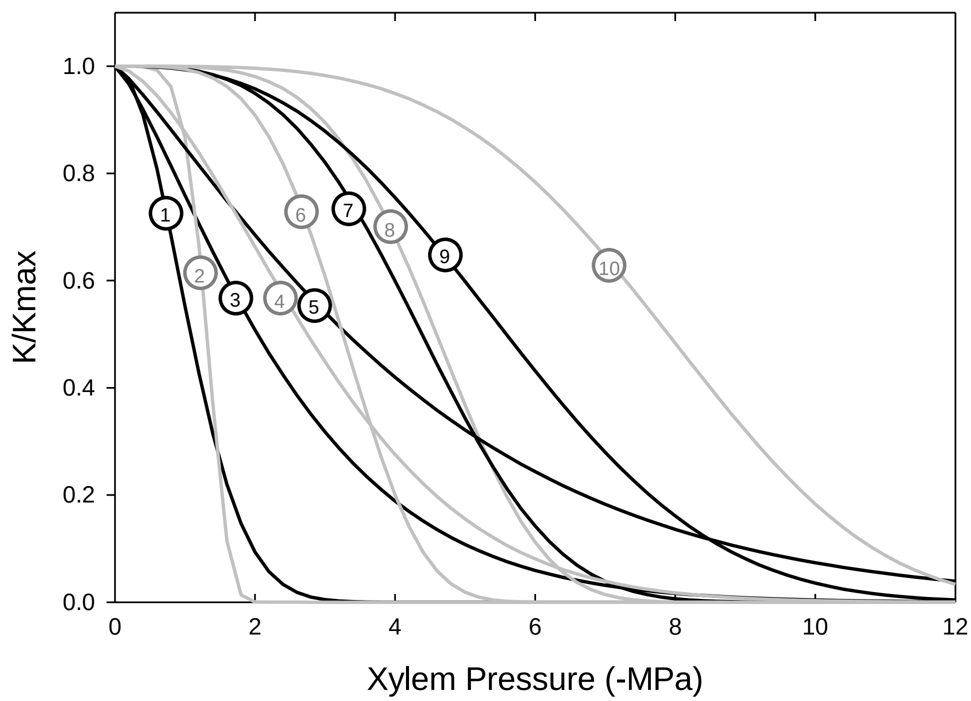

Methods S1 Model fitting

Prior drought. The importance of prior drought was estimated from experiments on the model. The model was driven by a data set to generate G and P_{canopy} outputs, using the extreme P_{soil} of the data set as the prior drought input. The downhill simplex routine was then used to fit the model *without* prior drought to these pre-droughted G and P_{canopy} outputs (via adjustment of G_{max}, k_{max}, and % rhizosphere inputs). The mean absolute error between pre-droughted vs non-pre-droughted fits averaged less than 2.7% (error as percentage of mean pre-droughted G or P_{canopy}). Data sets tested were numbers 1 (*Cavanellesia*, stem P50 = 1.11 MPa), 5 (*Cojoba* dry, P50 = 2.80 MPa), & 9 (*Cojoba* transitional dry, P50 = 4.63 MPa; Fig. S1, Table S1); these were chosen to represent a wide range in cavitation resistance.

Downhill simplex algorithm. This algorithm requires an initial 'simplex' defined by four sets of G_{max}, k_{max}, and % rhizosphere settings. Its performance was confirmed by fitting model output from the 'wrong' model input, converging to the correct values within 0.2%. To confirm a true global minimum was achieved when fitting data sets, the simplex was started from different settings. Only in a few cases (<10%) was this actually necessary.

Fig. S2 Sigmoid (Weibull c=3, b varied as shown) and exponential (c=1, b varied as shown) vulnerability curves tested in the sensitivity analysis of Figs S3 and S4.

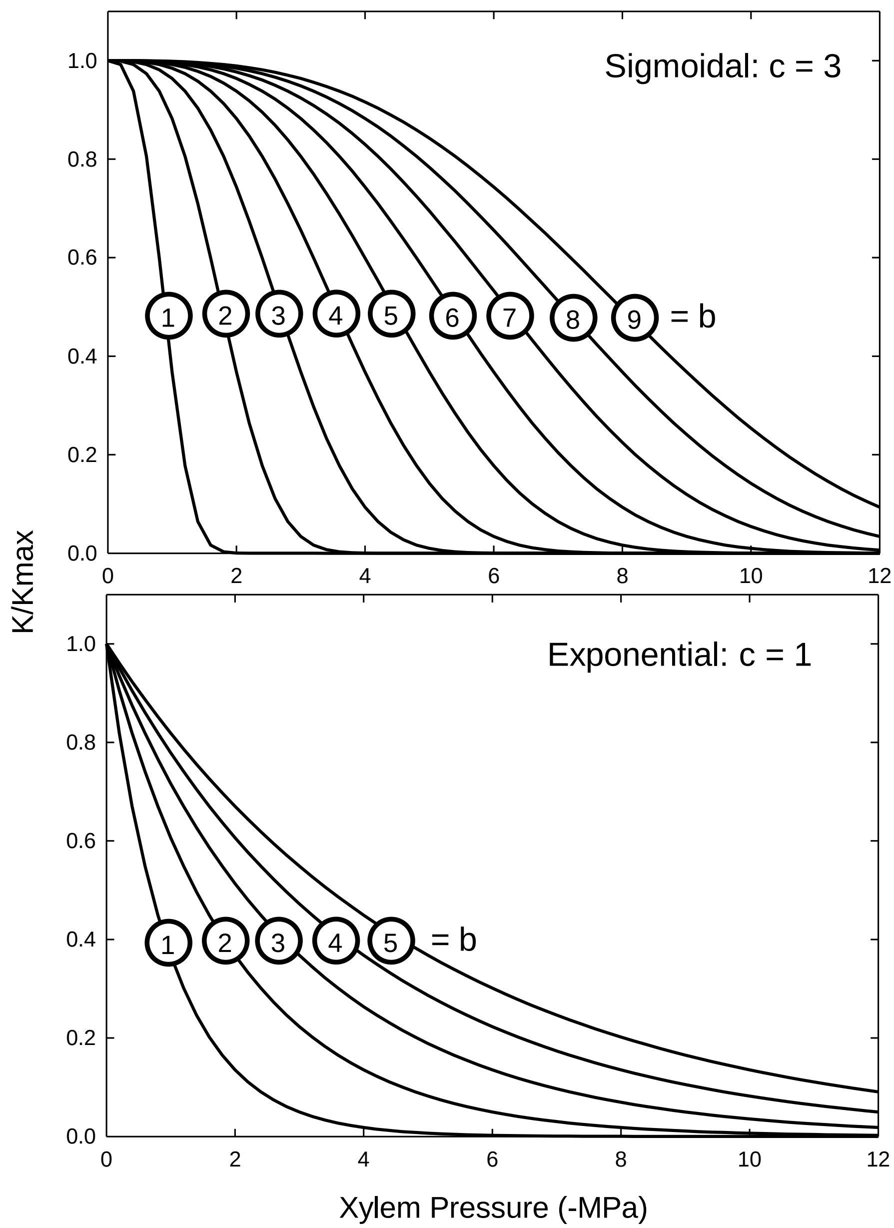

Fig. S3 Sensitivity of G to D. In each panel, all inputs were held at default settings (Table 1) except the input indicated. (a) Increasing the ratio of G_{max} to k_{max} (as labeled on curves) increased the closure response to D. (b) Drier soil (greater absolute P_{soil} as labeled) also increased the closure response to D. Inset shows the effect of exposure to *prior* drought (to the indicated P_{soil}) on depressing G when P_{soil} has returned to 0 (all Inset curves are at P_{soil} = 0). This resulted from irreversible cavitation during the drought; there was no prior drought effect when cavitation was reversible. (c) More vulnerable sigmoid vulnerability curves (P50 as labeled; Fig. S2) increased the closure response to D. (d) More vulnerable exponential curves (P50 as labeled; Fig. S2) also increased the closure response. Exponential curves produced immediate closure at lowest D, lacking the threshold response caused by sigmoid curves.

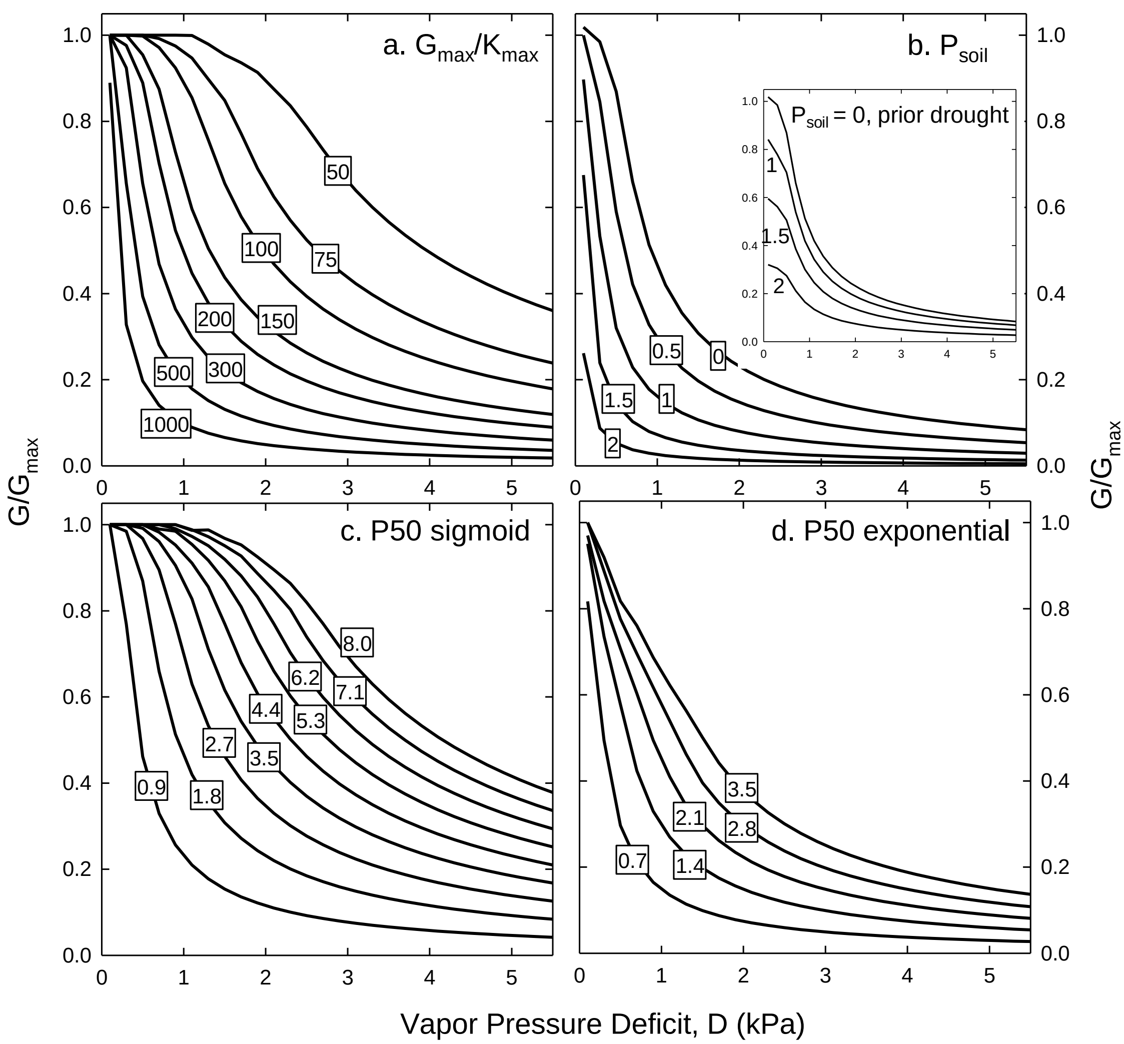

Fig. S4 Sensitivity of G to P_{soil}. In each panel, all inputs were held at default settings (Table 1) except the input indicated. (a) Increasing the ratio of G_{max} to k_{max} (as labeled on curves) increased the rate of stomatal closure, but without changing the P_{soil} at complete closure. (b) Greater % rhizosphere resistance increased closure from P_{soil}, while also restricting P_{soil} at complete closure. (c) More vulnerable sigmoid vulnerability curves (P50 as labeled) increased the closure response and restricted P_{soil} at complete closure. (d) More vulnerable exponential curves (P50 as labeled) increased closure, but the closure occurred at a slower rate than for the sigmoidal case, owing to the long tail on the exponential curve (Fig. S2).

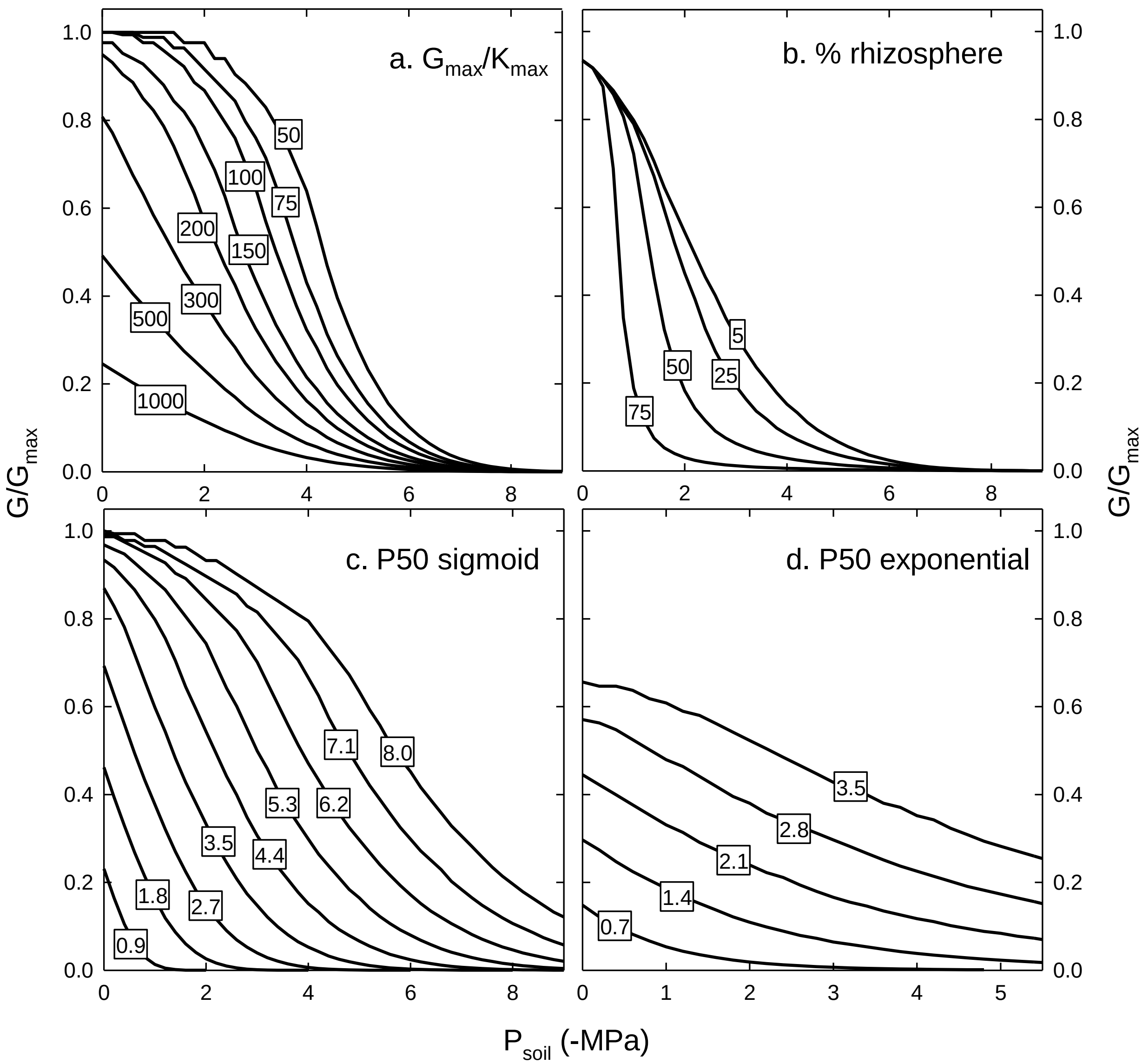

Fig. S5 Fig. 6 in the text, but with unlimited G_{max}. Maximum intercepts increased because they were no longer limited by G_{max}. Slopes became solely a function of the Weibull 'c' parameter.

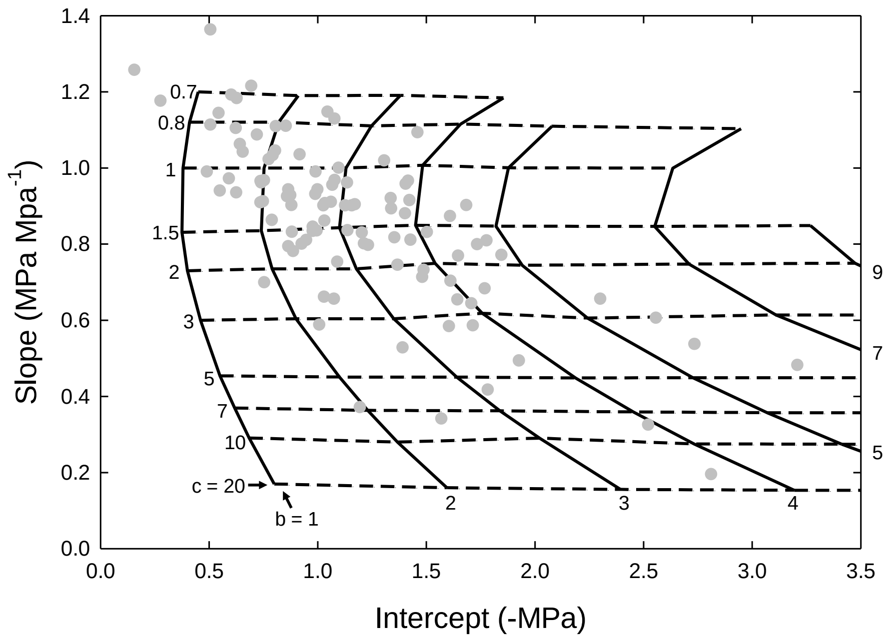

Fig. S6 The effect of the % rhizosphere setting (5, 25, 50% heavy curves) on the midday vs predawn P_{canopy} relationship. A single Weibull b=2 setting is shown, for c = 0.7 to 20 (dashed lines). The default 5% rhizosphere setting had a minimum slope of ca. 0.2 (as in Fig. S5). Increasing the % rhizosphere resistance dropped the minimum slope to zero and below. The intercept was minimally altered.

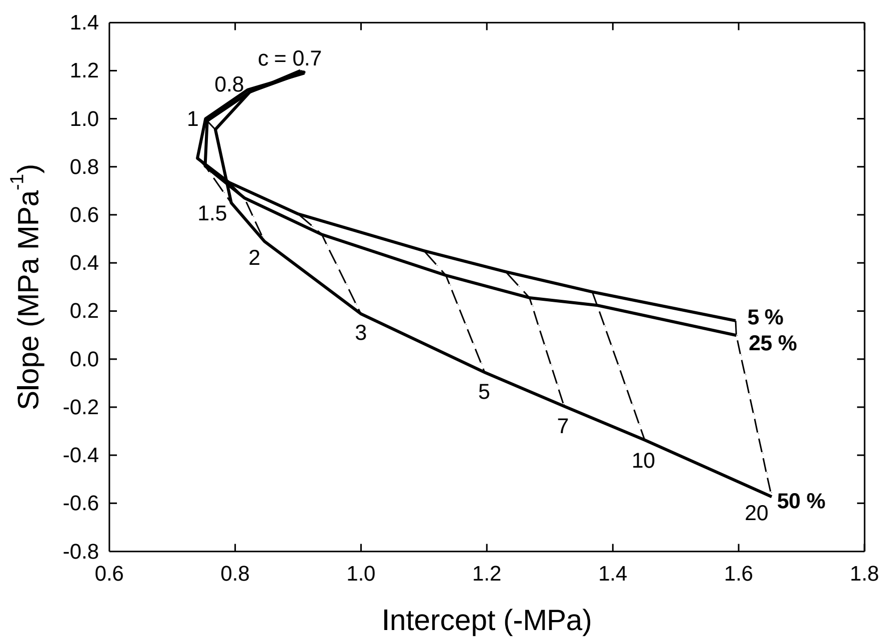

Fig. S7 Sequence of observed (closed symbols) and modeled (open symbols) canopy conductance (G) and P_{canopy}. Model set to irreversible cavitation. Measurements were made every 3–6 wk from November 2011 to July 2013, through two wet and two dry seasons in Panama. (a) *Annona hayesii* G. (b) *A. hayesii* P_{canopy}. (c) *Astronium graveolens* G. (d) *A. graveolens* P_{canopy}.

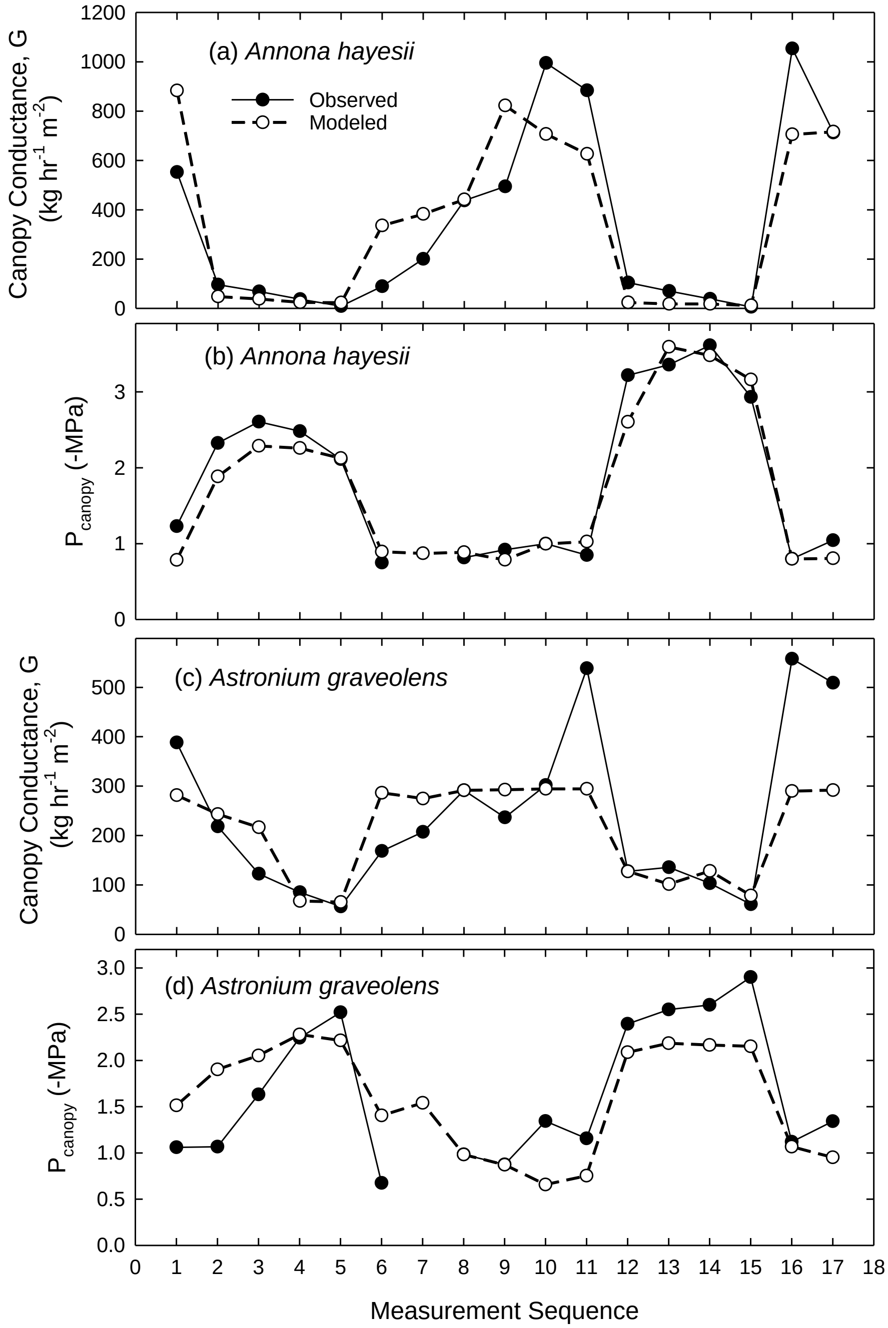

Fig. S8 Sequence of observed (closed symbols) and modeled (open symbols) canopy conductance (G) and P_{canopy}. Model set to irreversible cavitation. Measurements were made every 3–6 wk from November 2011 to July 2013, through two wet and two dry seasons in Panama. (a) *Bursera simaruba* G. (b) *B. simaruba* P_{canopy}. (c) *Cavanillesia platanifolia* G. (d) *C. platanifolia* P_{canopy}.

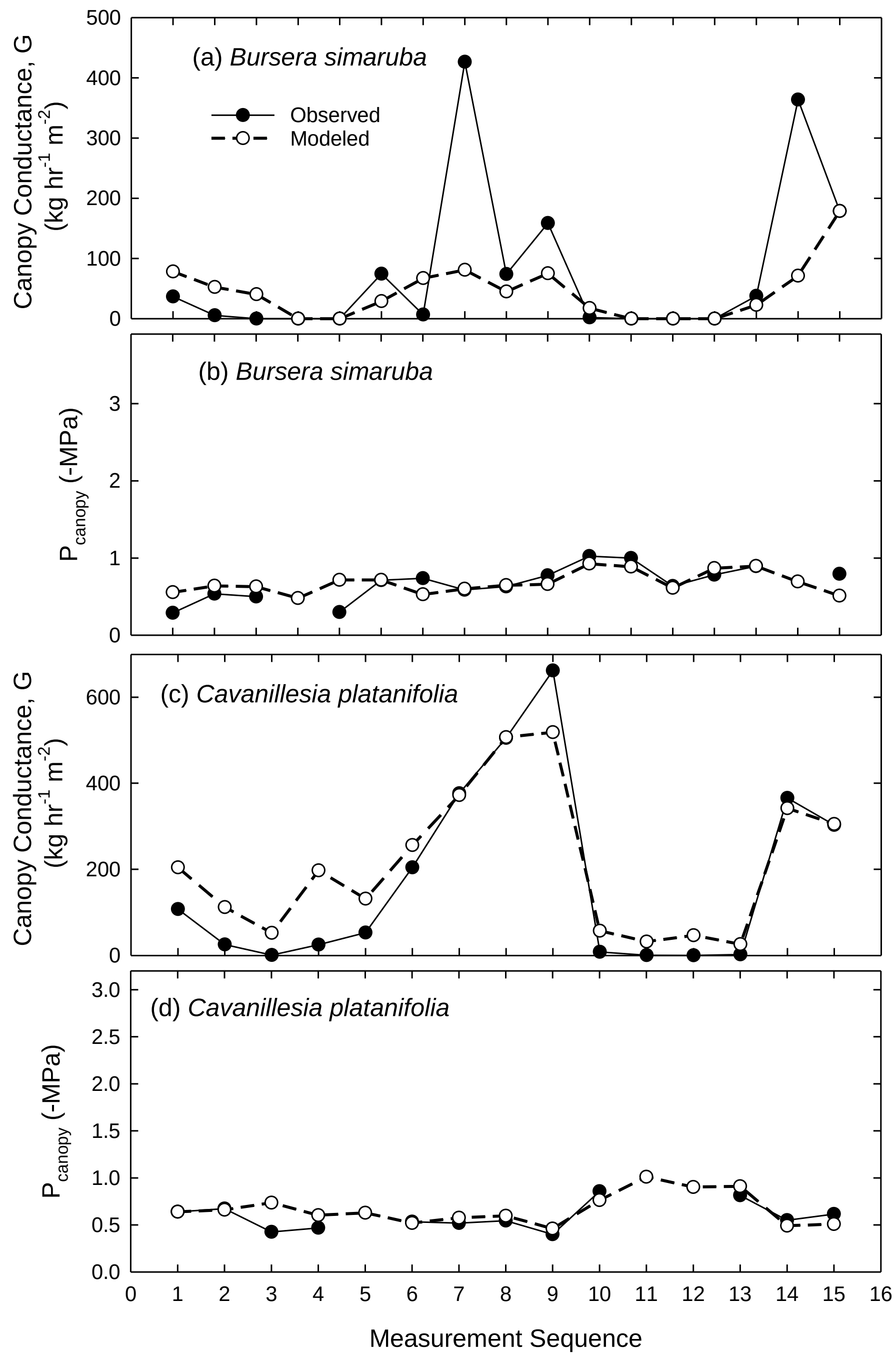

Fig. S9 Sequence of observed (closed symbols) and modeled (open symbols) canopy conductance (G) and P_{canopy}. Model set to irreversible cavitation. Measurements were made every 3–6 wk from November 2011 to July 2013, through two wet and two dry seasons in Panama. (a) *Cojoba rufescens* (dry forest) G. (b) *C. rufescens* (dry forest) P_{canopy}. (c) *C. rufescens* (transitional dry forest) G. (d) *C. rufescens* (transitional dry forest) P_{canopy}.

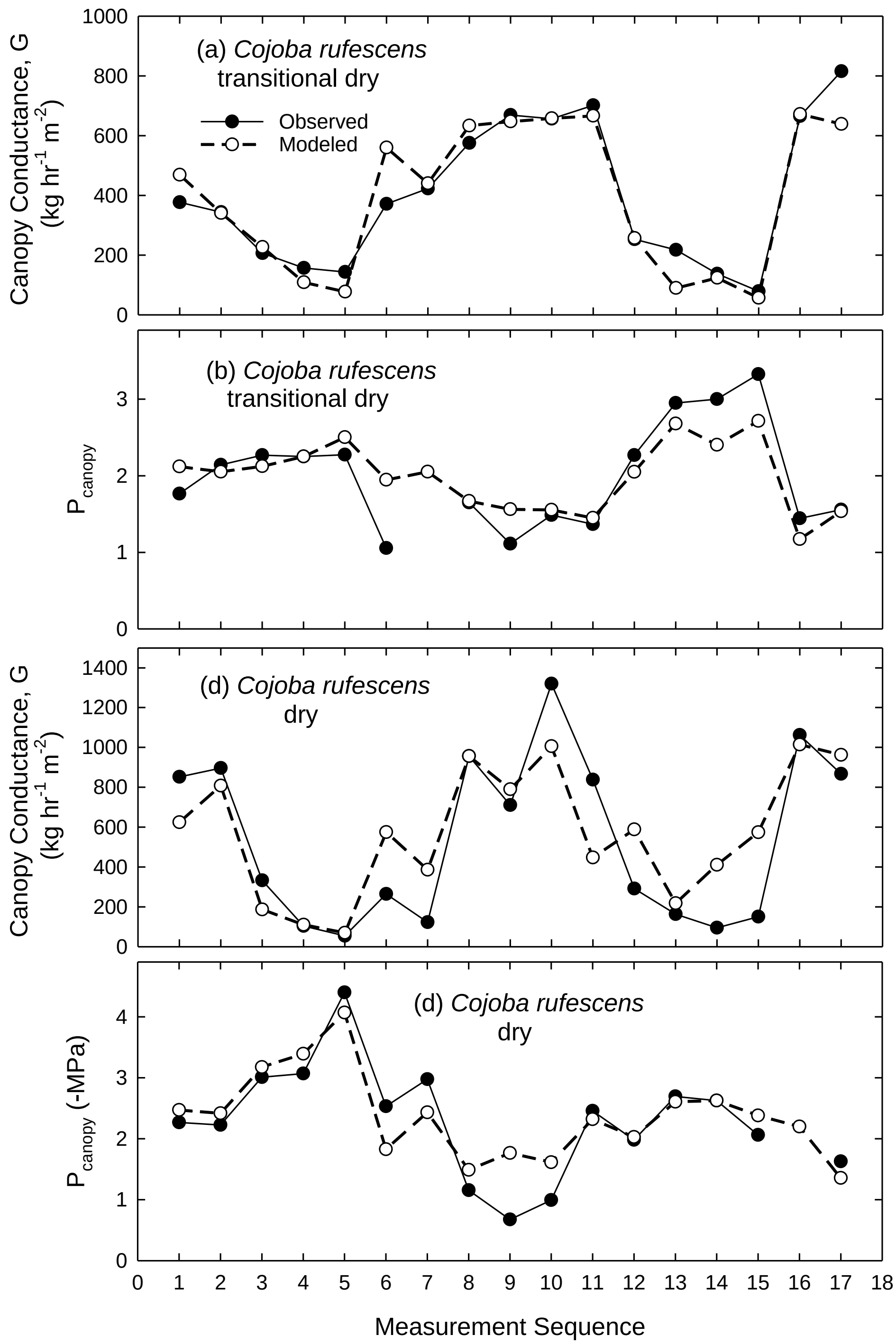

Fig. S10 Sequence of observed (closed symbols) and modeled (open symbols) canopy conductance (G) and P_{canopy}. Model set to irreversible cavitation. Measurements were made every 3–6 wk from November 2011 to July 2013, through two wet and two dry seasons in Panama. (a) *Genipa americana* G. (b) *G. americana* P_{canopy}.

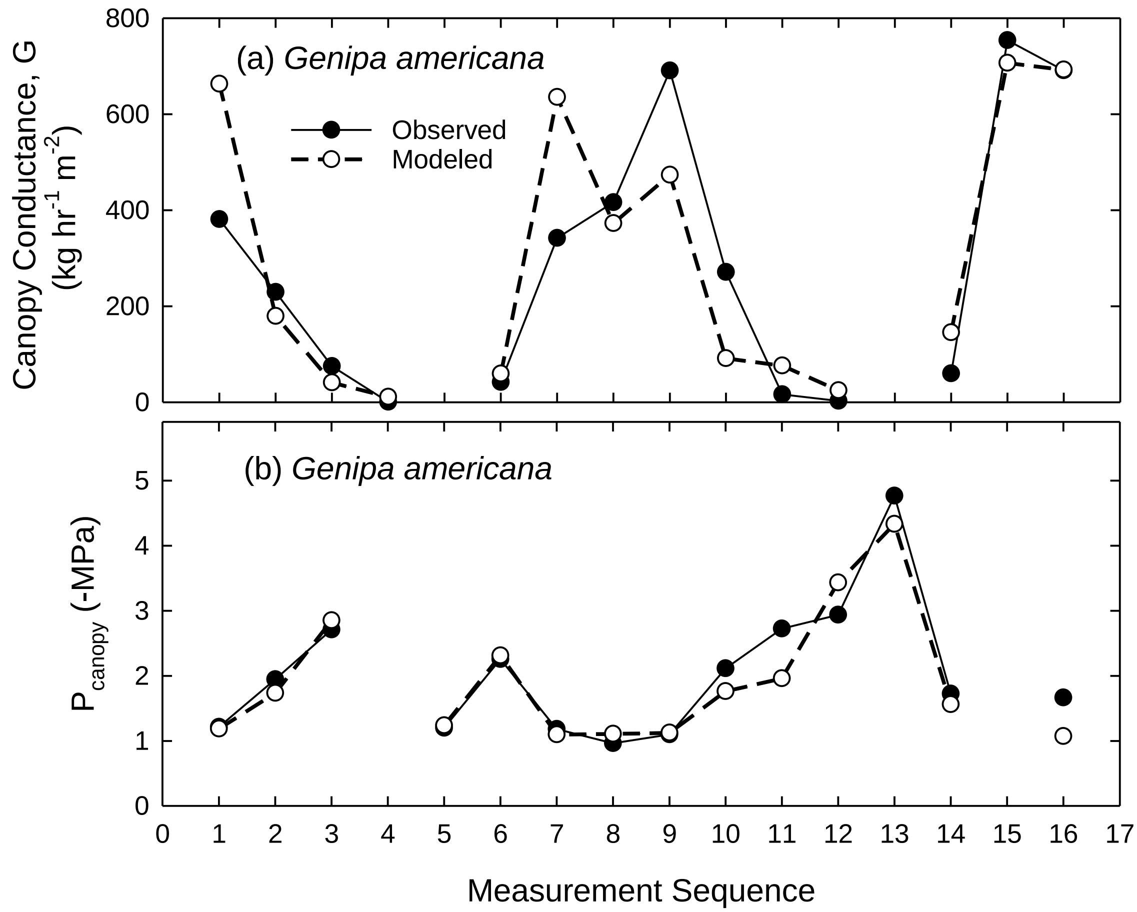

Fig. S11 Sequence of observed (dashed black) and modeled (grey) canopy conductance (G) and P_{canopy} for *Juniperus monosperma* and *Pinus edulis*. Model set to irreversible cavitation. An average of 8 measurement days were spaced over the 7 month (April–October) growing season for 2007-2010. The model was run on 6 trees per species, each tree shown sequentially and demarked by vertical blue lines. Each growing season per tree was fit separately. The final three *P. edulis* trees and last *J. monosperma* tree died after two growing seasons.

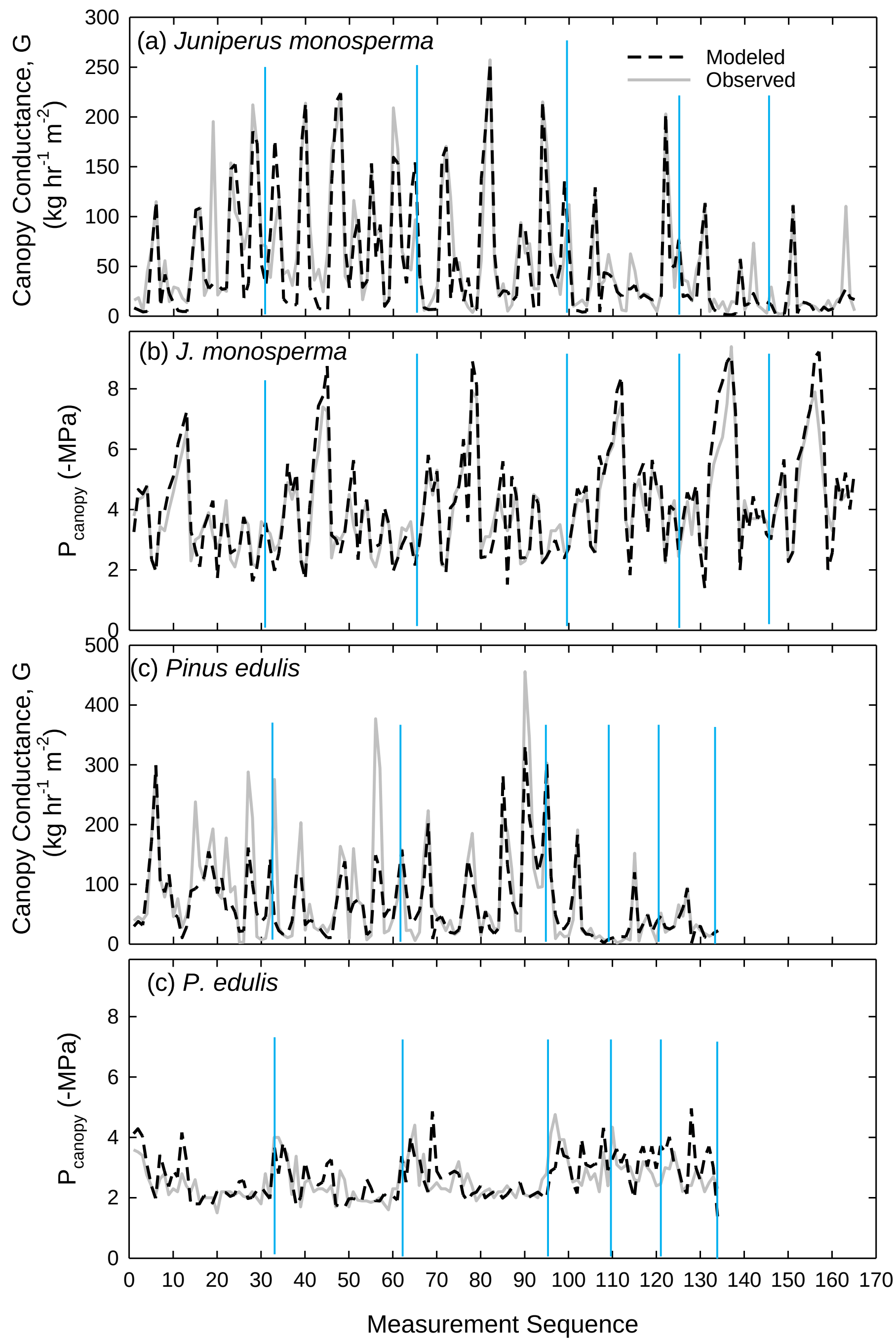

Table S2 Model fit statistics, fitting parameters, average observed G and plant hydraulic conductance (G_{ave}, k_{ave}), and stem P50's for 9 data sets as plotted in Fig. 9. Model was run in reversible cavitation mode.

Data Set	**P_{canopy} error[1]**		**G error[1]**		P r^2	G r^2	sample size	**G_{max}** **G_{ave}[4]**	SD+[5]	**k_{max}** **k_{ave}[4]**	SD+[5]	**%** rhiz	**P50[6]**
	mean	**%**	**mean**	**%**									
Annona hayesii, transitional dry[2]	0.21	11.4	128.6	37.3	0.94	0.76	P: 16 G:17	963 344	1.7	14.8 5.1	5.1	82	4.59
Astronium graveolens, transitional dry[2]	0.32	19.4	87.9	36.4	0.67	0.51	P: 16 G:17	245 242	0.02	3.3 4.8	-0.3	44	4.38
Bursera simaruba, dry[2]	0.13	18.4	59.8	74.4	0.35	0.30	P: 15 G:17	370 80	2.2	100 20.8	2.8	77	1.31
Cavanillesia platanifolia, transitional dry[2]	0.09	14.8	47.1	26.8	0.41	0.96	P:12 G:15	849 176	3.1	32.8 10.6	2.0	65	3.10
Cojoba rufescens, transitional dry[2]	0.27	13.5	54.0	13.5	0.73	0.90	P:16 G:17	740 400	1.4	6.2 5.4	0.2	56	4.63
C. rufescens, dry[2]	0.34	14.7	226	42.3	0.78	0.54	P:16 G:17	1289 534	1.8	14.5 15.9	-0.1	71	2.80
Genipa americana, dry[2]	0.31	15.0	74.7	26.3	0.87	0.54	P:14 G:14	869 284	2.1	17.5 9.5	0.9	69	2.04
Juniperus monosperma[3]	0.50	12.5	18.6	32.8	0.75	0.87	P:165 G:165	183 57	2.2	7.55 2.23	2.0	67	7.90
Pinus edulis[3]	0.47	18.4	28.2	36.7	0.30	0.71	P:134 G:134	591 77	5.9	10.3 4.0	1.3	40	2.75

[1]Mean absolute error, and its percentage of the observed mean; P_{canopy} in –MPa, G in kg h^{-1} m^{-2}.

[2]'Dry' and 'transitional' refer to the forest type; B. Wolfe *et al.* (unpublished).

[3]McDowell *et al.* (2013).

[4]G_{ave} and k_{ave} are observed averages in the data sets.

[5]SD+ is number of standard deviations that G_{max} or k_{max} is above their measured means.

[6]P50 is in –MPa.

Fig. S12 Modeled vs measured G (a, b) and P_{canopy} (c, d) for the seven tropical (a, c) and two piñon-juniper (b, d) data sets. Reduced major axis regressions shown for each data set (colored lines) and the entire panel (black line), along with dashed 1:1 line. Light green, *Annona*; cyan, *Astronium*; yellow, *Bursera*; blue, *Cavanillesia*; pink, *Cojoba* transitional dry; grey, *Cojoba* dry; red, *Genipa*; dark green, *Juniperus*; dark red, *Pinus*. Model was set to reversible cavitation.

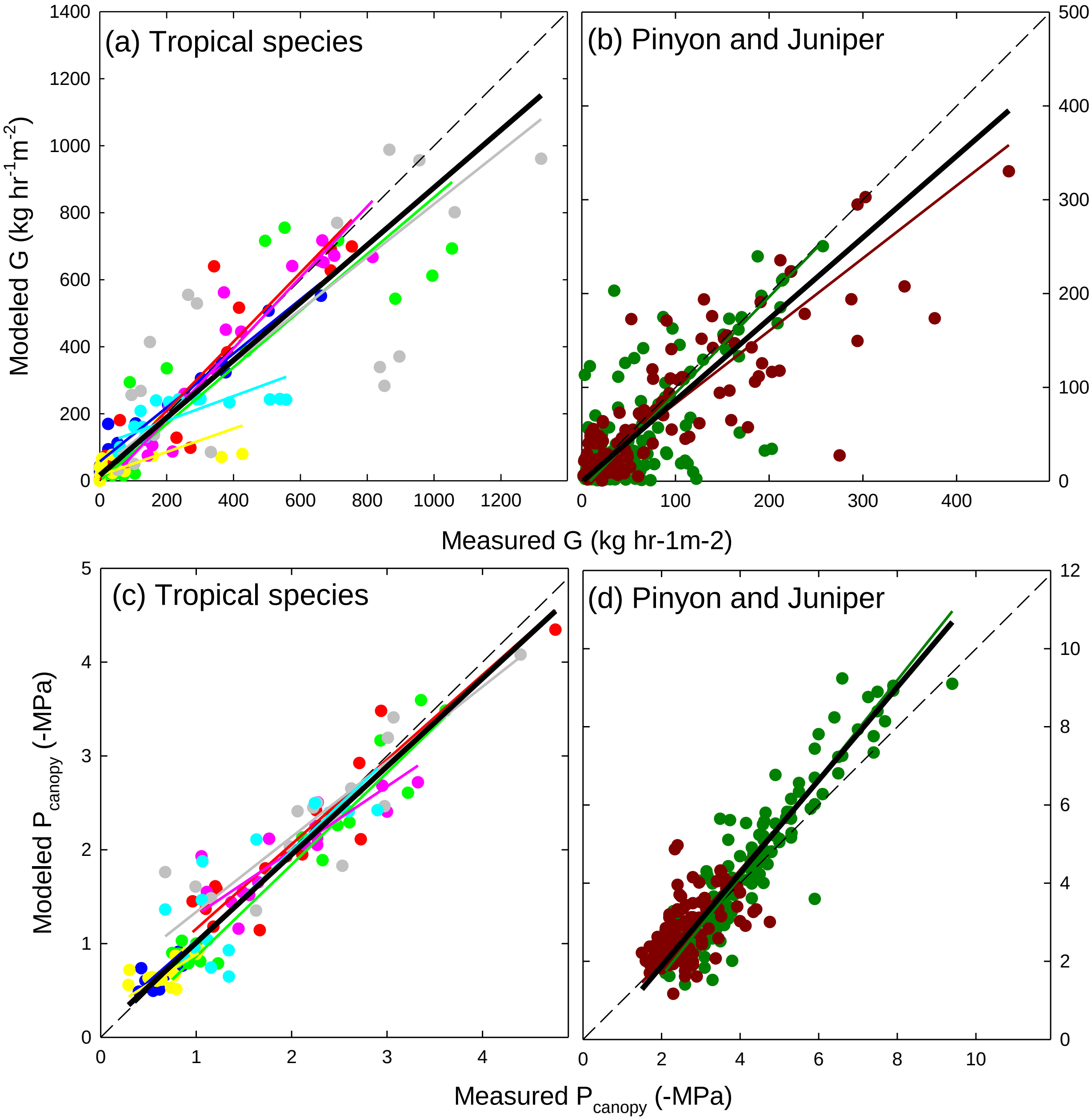

Notes S1 Model experiments on % rhizosphere compensation

The ability of % rhizosphere setting to compensate for missing xylem segmentation was tested in data sets 1 (*Cavanellesia*, stem P50 = 1.11 MPa), 5 (*Cojoba* dry, P50 = 2.80 MPa), & 9 (*Cojoba* transitional dry, P50 = 4.63 MPa; Fig. S1, Table S1). These sets were chosen to represent a wide range in cavitation resistance. For each data set, the model was segmented, assuming the leaf and root xylem P50 was 50% of the stem value (via adjustment of the Weibull b parameter only). The rhizosphere was set to the default of 5%, and G_{max} and k_{max} were set to best fit values (from Table 1). The model was driven by the data set sequence of D and predawn pressure to generate 'true' segmented G and P_{canopy} outputs. The segmentation was then removed (all xylem was given the stem vulnerability curve), and the downhill simplex routine was used to fit the segmented G and P_{canopy} outputs (via adjustment of G_{max}, k_{max}, and % rhizosphere inputs). The fitting reduced the average absolute error in P_{canopy} from 19.6% to 4.9% (% of mean segmented value), and average G error from 144.1% to 25.3%. The best-fit % rhizosphere rose an average of 1417% from 5% to 76%. Best fit G_{max} and k_{max} fell an average of 2.3% and 22.1%. The largest best-fit error was for G (45%) in the most vulnerable species (1, *Cavanellesia*), reflecting the fact that the % rhizosphere setting has the most effect in dry soils, by which point *Cavanellesia* was already shut down by cavitation.

References

McDowell NG, Fisher RA, Xu C, Domec JC, Hölttä T, Mackay DS, Sperry JS, Boutz A, Diskman L, Geheres N *et al*. 2013. Evaluating theories of drought-induced vegetation mortality using a multimodel-experimental framework. *New Phytologist* **200**: 304–321.